Particles I

Access the latest eBook →

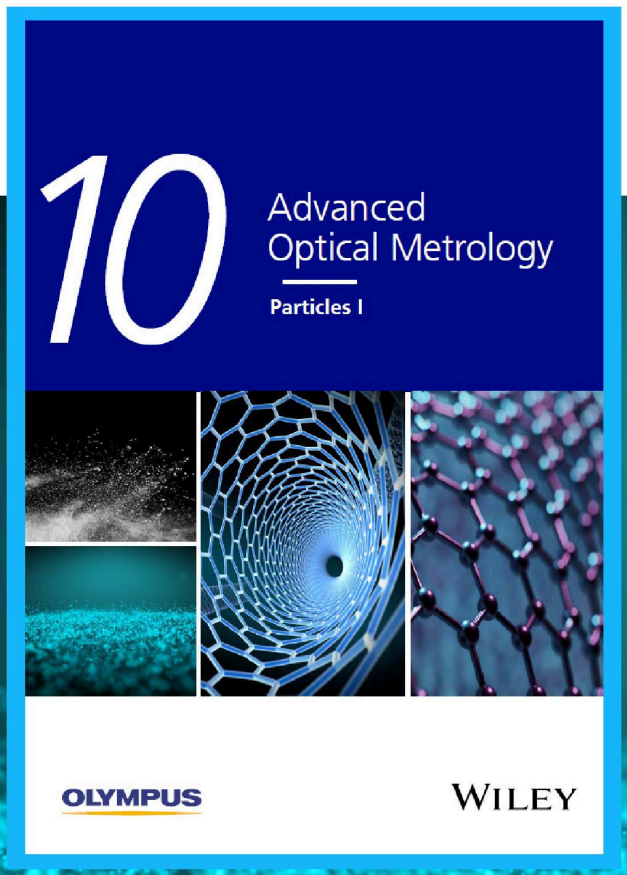

Particles: Unique Properties, Uncountable Applications

Read the latest eBook and better your knowledge with highlights from the recent studies on the design and characterization of micro- and nanoparticles for different application areas.

Access Now

This eBook is sponsored by

OLYMPUS

WILEY

Magnetocapacitance and Magnetoresistance Near Room Temperature in a Ferromagnetic Semiconductor: La_2NiMnO_6**

By *Nyrissa S. Rogado*, *Jun Li*, *Arthur W. Sleight*, and *Mas A. Subramanian**

Materials that show various responses to multiple external stimuli enable novel device applications. The behavior of systems with strong coupling between magnetic and electronic degrees of freedom provides both challenges for solid-state theory as well as novel phenomena for applications such as colossal magnetoresistance in perovskite manganites. Similarly, a strong coupling between magnetism and dielectric properties in magnetic insulators or semiconductors should lead to devices based on the magnetodielectric effect, where the dielectric properties can be controlled by a magnetic field. Large magnetic-field-induced changes in the resistivity and dielectric properties of La_2NiMnO_6 are found at temperatures as high as 280 K. This is a much higher temperature than previously observed for such a coupling between the magnetic, electric, and dielectric properties in a ferromagnetic semiconductor. The ferromagnetism of La_2NiMnO_6 was confirmed through neutron-diffraction studies. La_2NiMnO_6 is a rare example of a single-material platform with multiple functions, in which the spins, electric charge, and dielectric properties can be tuned by magnetic and/or electric fields.

Spintronics (short for spin electronics) is a new technology that combines electronics with magnetics through the manipulation of electron spins. It offers the potential for nonvolatile memories, faster data processing speeds with less power usage, larger storage densities, and additional functionalities, such as quantum computation, which are not possible with conventional semiconductor devices.[1,2] Present spintronic devices, e.g., the giant magnetoresistor (GMR), used in read-head sensors, consist of ferromagnetic metallic alloys wherein spin-dependent scattering and tunneling effects have been successfully applied for commercial use. However, in order to fully achieve the potential of practical spintronic devices, the next generation of spintronic materials should be based on ambient-temperature ferromagnetic semiconductors or heterostructures incorporating ferromagnetic metals with nonmagnetic semiconductors, which enable their easy integration into existing electronic devices. The search for semiconducting materials that exhibit strong ferromagnetic behavior at or above room temperature has been extremely difficult due to conflicting requirements in the crystal structure, chemical bonding, and electronic properties of semiconductors and ferromagnetic materials.[1,3]

Generally, ferromagnetic semiconductors and insulators only exhibit magnetic ordering at very low temperatures, e.g., EuS (Curie temperature, $T_c = 16$ K),[4] EuO ($T_c = 77$ K),[5] $CdCr_2Se_4$ ($T_c = 130$ K),[6] $BiMnO_3$ ($T_c = 100$ K),[7] $SeCuO_3$ ($T_c = 25$ K),[8] and diluted magnetic semiconductors, such as (Ga,Mn)As,[1] which precludes their use in devices. However, one exception is an ordered double perovskite, $La_2Ni^{2+}Mn^{4+}O_6$, an apparent ferromagnetic semiconductor that has a Curie temperature very close to room temperature ($T_c \sim 280$ K);[9–12] this is in the range where devices can be built with commercially available solid-state thermoelectric (Peltier) coolers.

Earlier studies on La_2NiMnO_6 were focused on verification of Goodenough–Kanamori's (GK) rules,[13] which predict that ferromagnetism results when an empty d orbital of one metal site interacts with a half-filled d orbital of another metal site through an anion in a 180° superexchange interaction. These rules assume that the interaction of e_g orbitals will dominate over interactions between t_{2g} orbitals due to the greater cation–anion overlap in the case of the e_g orbitals. Actually, the prediction of these rules was generally violated for double perovskites. For A_2MReO_6 (A = Ba, M = Fe, Mn, or Ni),[14] A_2FeMoO_6 (A = Sr, Ba),[15] and $ALaMnRuO_6$ (A = Sr, Ba), the coupling between the two transition-metal cations is, in fact, antiferromagnetic despite the fact that the e_g interaction should give ferromagnetism in all of these cases.[16] Instead, it is the t_{2g} interaction that dominates, giving rise to ferrimagnetism in these compounds. Sleight rationalized this behavior on the basis of energies of the t_{2g} levels for the two cations being much more similar than the energies of the e_g levels.[14] This violation of the GK rules is a direct result of coupling a 3d cation with a 4d or 5d cation. The GK rules, as originally set forth, might still apply if the two different cations were 3d cations and this seems to be confirmed in the artificially structured La_2FeCrO_6 double perovskite.[17] It was also suggested that La_2NiMnO_6 is a ferromagnetic semiconductor with ordered Ni^{2+} (d^8: $t_{2g}^6e_g^2$) and Mn^{4+} (d^3: $t_{2g}^3e_g^0$) ions occupying the metal (M) centers of corner-sharing MO_6 octahedra in a distorted perovskite structure (Fig. 1a). While studies using ^{55}Mn NMR and X-ray absorption spectroscopy support the presence of Ni^{2+}/Mn^{4+} ordering in this material,[18–20] two neutron-diffraction studies disagree about whether the oxidation states are Ni^{2+}/Mn^{4+} or Ni^{3+}/Mn^{3+}.[21,22] The structure of La_2NiMnO_6 is rhombohedral ($R\bar{3}$) at high temperatures and transforms to monoclinic ($P2_1/n$) at low temperatures. These two structures typically coexist over a significant temperature range, which includes room temperature.[12] The coexistence

[*] Dr. M. A. Subramanian, Dr. N. S. Rogado
DuPont Central Research and Development, Experimental Station
P.O. Box 80328, Wilmington, DE 19880-0328 (USA)
E-mail: Mas.Subramanian@usa.dupont.com
Dr. J. Li, Prof. A. W. Sleight
Department of Chemistry, Oregon State University
Corvallis, OR 97331 (USA)

[**] We thank C. Y. Jones and B. H. Toby of the National Institute of Standards and Technology, U.S. Department of Commerce for providing the neutron diffraction data. We also acknowledge valuable discussions with P. M. Woodward concerning the magnetic structure. Supporting Information is available online from Wiley InterScience or from the author.

 DOI: 10.1002/adma.200500737

ADVANCED MATERIALS

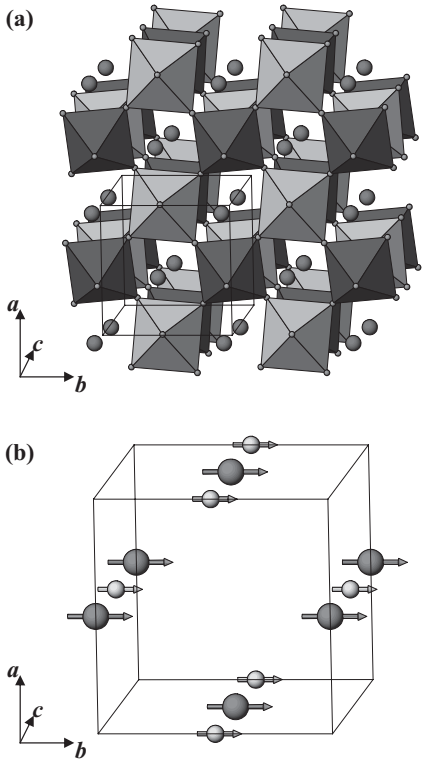

Figure 1. a) Atomic and b) magnetic structures of La_2NiMnO_6. In (a), dark and light polyhedra are shown for MnO_6 and NiO_6, respectively; large and small spheres are La^{3+} and O^{2-}, respectively. In (b), large spheres are Mn^{4+} (d^3, $t_{2g}^3e_g^0$, $\mu Mn = 3.0(2)\,\mu_B$), small spheres are Ni^{2+} (d^8, $t_{2g}^6e_g^2$, $\mu Ni = 1.9(3)\,\mu_B$), magnetic moments are aligned along the *b*-axis. μMn, μNi are the magnetic moments on the Mn, Ni sites, respectively. μ_B is the Bohr magneton (9.27×10^{-24} Am^2).

of structures is presumably related to local inhomogeneities due to the fact that this phase exists over a range of Ni/Mn ratios and that there is a small amount of antisite disorder on the Ni/Mn sites.

Single-phase samples of La_2NiMnO_6 were prepared using conventional solid-state synthetic methods. Powder X-ray diffraction was used to characterize the samples. Neutron powder diffraction data were obtained from the Center for Neutron Research at the National Institute of Standards and Technology (NIST). Details of data collection and analysis are given in the Supporting Information. The sample was a mixture of the $P2_1/n$ and $R\bar{3}$ structures at room temperature but was 100 % $P2_1/n$ at 3.5 K. On cooling the sample from room temperature to 3.5 K, no new peaks were observed on magnetic ordering, as would be expected if the ordering were ferromagnetic. Significant increases in intensity were observed for some peaks, most notably the (200) peak based on the pseudocubic cell. The intensity due to the magnetic ordering could only be fitted assuming ferromagnetic order. A least-squares refinement of the magnetic moments gave a moment of $3.0(2)\,\mu_B$ on the Mn site and $1.9(3)\,\mu_B$ on the Ni site, which are in good agreement with the values of 3.0 and 2.0 expected for Mn^{4+} and Ni^{2+}, respectively. The spins are parallel to the *b*-axis (Fig. 1b). Refinement of atomic positions gave three Ni–O–Mn angles in the range 159 to 162°. Despite this deviation from 180°, the expectations of the GK rules for a 180° interaction are realized.

The magnetization measurements were taken both as a function of temperature at fixed fields and as a function of applied magnetic field at fixed temperatures. The magnetic susceptibility, $\chi(T)$, of La_2NiMnO_6 in an applied field of 1 T is shown in Figure 2. $\chi(T)$ shows a magnetic transition at ~280 K, indicating the onset of ferromagnetic long-range ordering, and agreeing well with the literature. The inverse susceptibility ($1/\chi$) plot is also shown in the figure as an inset. The high-temperature data, from 300 to 320 K, were fitted to

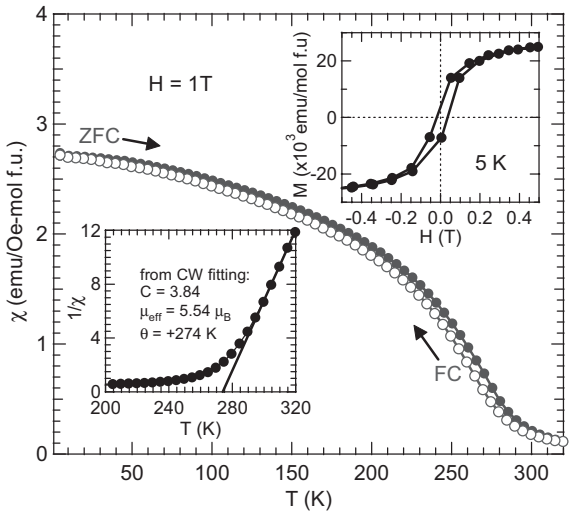

Figure 2. Magnetic susceptibility $\chi(T)$ at 1 T on zero-field (ZFC) and field cooling (FC). Insets show a plot of $1/\chi$ versus *T* fitted to the Curie–Weiss law (lower left) and field-dependent magnetization data at 5 K (upper right). *C*: Curie constant, in units of emu K mol^{-1}; θ: Weiss constant; μ_{eff}: effective paramagnetic moment; *M*: magnetization; *H*: field strength.

the Curie–Weiss law from which *C* and θ were determined. The parameters obtained from the present Curie–Weiss fit should only be taken as an approximation, because the small temperature range used is very close to the magnetic-ordering temperature. The Curie–Weiss fit to the $1/\chi$ data of La_2NiMnO_6 yielded $C = 3.84$ emu K mol^{-1} f.u. (f.u. = formula unit) and $\theta = +274$ K. The large positive θ value indicates strong ferromagnetic interactions between the Ni^{2+} and Mn^{4+} spins. The effective paramagnetic moment was calculated to be $5.5\,\mu_B$, which is less than the simple prediction of a spin system with non-interacting electron spins ($\mu_{calc} = 5.92\,\mu_B$).

The field dependence of the magnetization of La_2NiMnO_6 is also shown in Figure 2 as an inset. The *M* versus *H* plot shows a small magnetic hysteresis ($H_C \approx 300$ Oe; 1 Oe = $1000/4\pi$ T) at 5 K. The highest saturated magnetization at 5 K and a 5 T applied field is ~27 700 emu mol^{-1} (equivalent to $4.96\,\mu_B$/f.u.), which is very close to the full magnetization of $5.0\,\mu_B$/f.u. expected for ferromagnetic $La_2Ni^{2+}Mn^{4+}O_6$.

The temperature- and field-dependent resistivities were measured using the four-wire method. La_2NiMnO_6 was found to be semiconducting with a high resistivity, $\sim 10^2\ \Omega$ cm at room temperature, which increases with decreasing temperature. At 200 K, this material shows a 3 % decrease in resistance in a 1 T field.

Figure 3 shows the temperature dependence of the dielectric constant, ε, of La_2NiMnO_6 at 10 kHz and at selected magnetic fields. At or above room temperature, the dielectric constant of La_2NiMnO_6 is approximately 600. At zero field, a

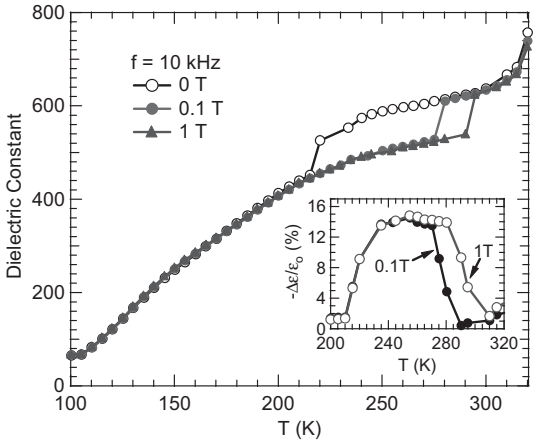

Figure 3. Temperature dependence of the dielectric constant at 10 kHz for 0, 0.1 and 1 T applied fields. Inset shows the magnetocapacitance effect ($-\Delta\varepsilon/\varepsilon_0$) with 0.1 and 1 T applied fields.

gradual decrease in the dielectric constant is observed with decreasing temperature until it reaches 220 K, below which ε decreases steeply. When a magnetic field is applied, this transition moves to higher temperatures, 280 K for a 0.1 T field and 295 K for a 1 T field. This shift results in a large change in the dielectric response of La_2NiMnO_6 in the vicinity of the transition temperature (270–280 K) in the presence of a magnetic field (Fig. 3, inset).

In summary, the appearance of both magnetoresistance and magnetocapacitance effects in the ferromagnetic semiconducting compound, La_2NiMnO_6, indicates coupling between the magnetic, electronic, and dielectric properties, which may be controlled by the application of magnetic fields. The fact that this behavior is observed very close to room temperature provides optimism for practical spintronic applications.

Experimental

Stoichiometric amounts of the metal nitrates were dissolved together in water. The solution was evaporated and the residue was dried at 400 K for 1–2 days. The resulting brown powder was ground, placed in a dense alumina crucible and heated in air at 875 K for 30 min, then at 1375 K for 16 h, and cooled slowly to room temperature. The powder sample was then ground, pressed into a pellet, heated at 1375 K for 16 h, and cooled slowly to room temperature. The sample was reground, repelletized and reheated several times until no further changes in the diffraction pattern were observed.

Powder X-ray diffraction with Cu Kα radiation and neutron diffraction were employed to characterize the crystal and magnetic structures of the samples. The magnetic, transport, and dielectric properties of the samples were characterized using a Quantum Design Physical Property Measurement System (PPMS). The magnetization measurements were taken both as a function of temperature at fixed fields, and as a function of applied magnetic field at fixed temperatures. Transport properties were measured from 320 to 200 K and from 0.0 to 1.0 T using the four-wire resistivity option of the PPMS. The samples for capacitance measurements were prepared by applying silver paint to opposite faces of the sintered pellet and attaching Cu wires to each face using silver epoxy. The capacitance was measured using a HP 4284 LCR meter. The dielectric measurements were done at various frequencies (10 kHz–1 MHz) with an excitation of 1 V from 100–320 K. The temperature and applied magnetic fields during the capacitance measurements were controlled by the PPMS.

Received: April 12, 2005
Final version: May 2, 2005
Published online: July 29, 2005

[1] S. A. Wolf, D. D. Awschalom, R. A. Buhrman, J. M. Daughton, S. von Molnar, M. L. Roukes, A. Y. Chtchelkanova, D. M. Treger, *Science* **2001**, *294*, 1489.
[2] G. A. Prinz, *Science* **1998**, *282*, 1660.
[3] D. D. Awschalom, M. E. Flatte, N. Samarth, *Sci. Am.* **2002**, *286*, 67.
[4] S. Van Houten, *Phys. Lett.* **1962**, *2*, 215.
[5] B. T. Matthias, R. M. Bozorth, J. H. Van Vleck, *Phys. Rev. Lett.* **1961**, *7*, 160.
[6] P. K. Baltzer, H. W. Lehmann, M. Robbins, *Phys. Rev. Lett.* **1965**, *15*, 493.
[7] T. Kimura, S. Kawamoto, I. Yamada, M. Azuma, M. Takano, Y. Tokura, *Phys. Rev. B* **2003**, *67*, 180 401.
[8] M. A. Subramanian, A. P. Ramirez, W. J. Marshall, *Phys. Rev. Lett.* **1999**, *82*, 1558.
[9] A. Wold, R. J. Arnott, J. B. Goodenough, *J. Appl. Phys.* **1958**, *29*, 387.
[10] J. B. Goodenough, A. Wold, R. J. Arnott, N. Menyuk, *Phys. Rev.* **1961**, *124*, 373.
[11] N. Y. Vasanthacharya, P. Ganguly, J. B. Goodenough, C. N. R. Rao, *J. Phys. C* **1984**, *17*, 2745.
[12] R. I. Dass, J.-Q. Yan, J. B. Goodenough, *Phys. Rev. B* **2003**, *68*, 064 415.
[13] a) J. B. Goodenough, *Phys. Rev.* **1955**, *100*, 564. b) J. Kanamori, *J. Phys. Chem. Solids* **1959**, *10*, 87.
[14] A. W. Sleight, J. F. Weiher, *J. Phys. Chem. Solids* **1972**, *33*, 679.
[15] F. Patterson, C. Moeller, R. Ward, *Inorg. Chem.* **1963**, *2*, 196.
[16] K. Ramesha, V. Thangadurai, D. Sutar, S. V. Subramanyam, G. N. Subbanna, J. Gopalakrishnan, *Mater. Res. Bull.* **2000**, *35*, 559.
[17] K. Ueda, H. Tabata, T. Kawai, *Science* **1998**, *280*, 1064.
[18] K. Asai, H. Sekizawa, S. Iida, *J. Phys. Soc. Jpn.* **1979**, *47*, 1054.
[19] M. Sonobe, K. Asai, *J. Phys. Soc. Jpn.* **1992**, *61*, 4193.
[20] M. C. Sanchez, J. Garcia, J. Blasco, G. Subias, J. Perez-Cacho, *Phys. Rev. B* **2002**, *65*, 144 409.
[21] J. Blasco, M. C. Sánchez, J. Pérez-Cacho, J. García, G. Subías, J. Campo, *J. Phys. Chem. Solids* **2002**, *63*, 781.
[22] C. L. Bull, D. Gleeson, K. S. Knight, *J. Phys. Condens. Matter* **2003**, *15*, 4927.

